Copyright IPCO-2014
Vol.2
ISSN : 2356-5608

Performance Optimization of a Photovoltaic Water-Pumping System

Kamal Himour [#1], Kaci Ghedamsi[#2], and El Madjid Berkouk[*3]

[#] *Laboratory of Renewable Energy Mastery, University of Bejaia, Algeria.*
Himour.kamal@hotmail.fr, kghedamsi@yahoo.fr
[*] *Control Process Laboratory, ENP of Algiers.*
emberkouk@yahoo.fr

***Abstract* – In this paper, we propose an optimization of dynamic performances for a pumping structure constituted by an induction motor coupled to a centrifugal pump. The considered system is supplied by a photovoltaic generator (GPV) through two static converters piloted in an independent manner. We use an intelligent approach for the improvement and optimization of the PV control performance based on fuzzy logic ensures the working of the GPV with its maximal power via the control of a buck-boost converter. And in order to generate the output voltages to the induction motor with very low distortion we use the Simplified Space Vector Modulation for a three-level diode clamped inverter (DCI). Also, we use the concept of vectorial control by rotor flux orientation and fuzzy logic controller for motor speed to pilot the working of the induction motor. Simulation results leads the proposed structure to the optimum operating condition and permits to localize the static limits of working in steady state and the dynamic regimes.**

***Keywords* – Photovoltaic Generator, Fuzzy Logic, three-Level Diode Clamped Inverter, Space Vector Modulation, Flux Oriented Control, Induction Motor, Centrifugal Pump**.

I. INTRODUCTION

The application of photovoltaic electromechanical system for water pumping has increased in remote areas of developing countries where the extension of the conventional electrical supply network would be impossible and expensive**.** In this work, the dynamic performances of a system which uses an induction motor connected to a photovoltaic (PV) generator through an inverter is studied and optimized**.**

The photovoltaic array is an unstable source of power since the peak power point depends on the temperature and the irradiation level. A maximum peak power point tracking is then necessary for maximum efficiency. In this work, a maximum power point tracker for photovoltaic panel is proposed. Fuzzy input parameters, dP / dV and variation of duty cycle (ΔD) , are used to generate the optimal MPP converter duty cycle, such that solar panel maximum power is generated under different operating conditions.

The output voltage waveforms in multilevel inverters can be generated at low switching frequencies with high efficiency and low distortion. In recent years, beside multilevel inverters various pulse width modulation (PWM) techniques have been also developed. Space Vector Modulation (SVM) technique is one of the most popular techniques gained interest recently. A new simplified space vector Modulation method for a three-level diode clamped inverter is proposed in this paper. As a cheaper alternative, this paper investigates the output quality and high level of multilevel inverter to match a photovoltaic generator to an induction motor for a water pumping structure.

The paper is organized as follow: in section II we presented the global model of the system: mathematical model of the photovoltaic generator, Power optimization of the PV generator by a fuzzy logic controller, Modelling and simplified SVM of the three- level diode clamped inverter, command of the induction motor by flux oriented control and fuzzy logic. Then, in section III we presented the simulation results for the global photovoltaic water pumping system for one day for a type village that's its daily consumptions is estimated by 70 m^3 and we terminated by a conclusion of this study in section IV.

II.GLOBAL SYSTEM MODELLING

The photovoltaic water-pumping system is composed by: PV generator, Buck-Boost converter, Fuzzy Logic Controller, Three-level DCI, Induction Motor and a Centrifugal Pump.

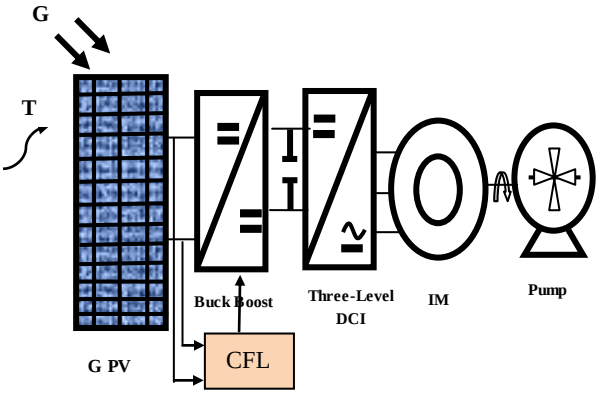

Fig.1 Global PV water pumping system.

A. *Modeling of the photovoltaic generator*

The equivalent circuit of a photovoltaic cell shown in Fig.2. It's widely used in literature [1].

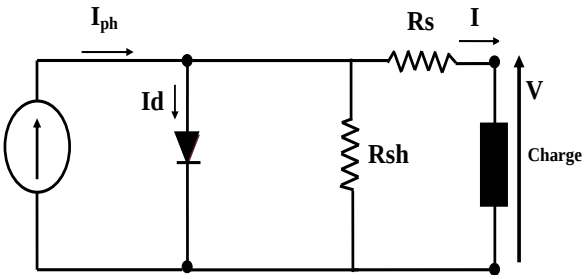

Fig. 2 Photovoltaic cell equivalent circuit.

Th current-voltage characteristic for a PV cell is :

$$I = I_{ph} - I_s\left[\left(\exp\frac{V + I.R_s}{m.\frac{K.T}{q}}\right) - 1\right] - \frac{V + I.R_s}{R_{sh}} \quad (1)$$

Where:

I_{ph}: the photo-current, I_s : the saturation current of diode, m: ideality factor, R_s and R_{sh} : series and parallel resistance, T : junction temperature, K : Boltzmann constant, q : electron charge.

B. *Power panel optimization by fuzzy logic*

The Principe of a fuzzy logic controller for a PV system is shown in Fig. 3 [2]:

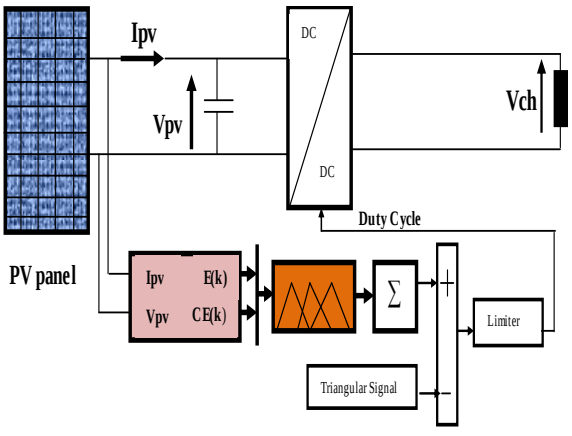

Fig.3 Fuzzy logic controller for a PV system.

1) *Fuzzification*

The actual voltage and current of PV panels can be measured continuously on A/D converter. We have focused on single input –single output plant in which control is determined on the basis of satisfaction of two criteria relating to two input variables error (E) and change error (CE) expressed as follows:

$$E(k) = \frac{P_{pv}(k+1) - P_{pv}(k)}{V_{pv}(k+1) - V_{pv}(k)} \quad (2)$$

$$CE(k) = E(k+1) - E(k) \quad (3)$$

Where $P_{pv}(k)$, $V_{pv}(k)$ are the power and voltage of the PV module, respectively there for $E(k)$ is zeros at the maximum power point of PV panel.

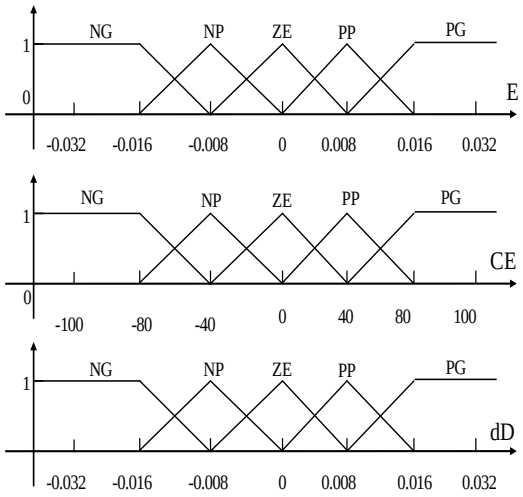

Fig. 4 Membership functions for E, CE and dD.

2) *Fuzzy Inference*

Table I Shows the rules of fuzzy controller, where all the entries of the matrix are fuzzy sets of error, change error and duty cycle dD of the chopper. The control rule must be designed in order that input variable E has to always be zeros.

TABLE I
TABLE RULE.

E(k) / CE(k)	NG	NP	ZE	PP	PG
NG	ZE	ZE	PG	PG	PG
NP	ZE	ZE	PG	PG	PG
ZE	PP	ZE	ZE	ZE	NP
PP	NP	NP	NP	ZE	ZE
PG	NG	NG	NG	ZE	ZE

3) *Defuzzification*

The final combined fuzzy set is defined by the union of all rule output fuzzy set using the maximum aggregation method .for a sampled data representation, the center of gravity dD_o is computed point wise by:

$$dD_0 = \frac{\sum \mu(D_j).D_j}{\sum \mu(D_j)} \quad (4)$$

C. *Model and control of the 3 level DCI*

A three-phase three-level diode-clamped inverter is shown in Fig.5 [3].Each leg is composed of two

upper and lower switches with anti-parallel diodes. Two series dc link capacitors split the dc bus voltage in half and six clamping diodes confine the voltages across the switch within the voltages of the capacitors.

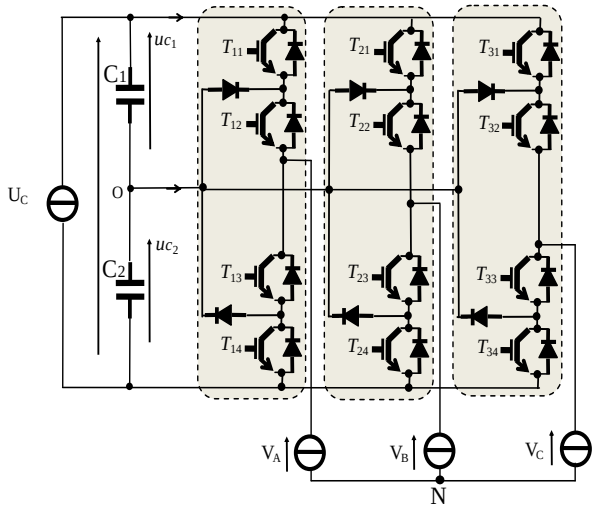

Fig.5 Three level diode clamped inverter (DCI).

1) Connection fonctions

For each leg of the inverter, we define three connection functions, each one is associated to one of the three states of the leg:

$$\begin{cases} F_{c1j} = F_{1j}.F_{2j} \\ F_{c2j} = F_{2j}.F_{3j} \\ F_{c3j} = F_{3j}.F_{4j} \end{cases} \quad (5)$$

TABLE III
STATES OF ONE LEG OF THE THREE LEVEL DCI.

F_{k1}	F_{k2}	F_{k3}	F_{k4}	V_k	Etat
0	0	1	1	-Uc/2	N
0	1	1	0	0	O
1	1	0	0	Uc/2	P
1	0	0	1	unknown	-

As indicated in table II, each leg of the inverter can have three possible switching states P,O N.

2) Output voltages

The output voltages of a three level diode clamped inverter are expressed as follows:

$$\begin{bmatrix} V_{10} \\ V_{20} \\ V_{30} \end{bmatrix} = \begin{bmatrix} F_{c11} & F_{c21} & F_{c31} \\ F_{c12} & F_{c22} & F_{c32} \\ F_{c13} & F_{c23} & F_{c33} \end{bmatrix} . \begin{bmatrix} \frac{Uc}{2} \\ 0 \\ \frac{-Uc}{2} \end{bmatrix} \quad (6)$$

Fig. 6 shows the space vector diagram of the three level inverter. The output voltage space vector is identified by combination of switching states P, O, N of the three legs. Since three kinds of switching states exist in each leg, three level inverter has $3^3 = 27$ switching states.

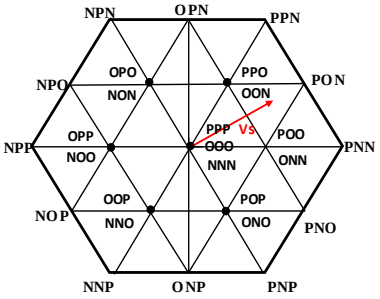

Fig.6 Three level diode clamped inverter space vector diagram.

3) Simplified Space vector modulation

In SVPWM method the output voltage is approximated by using the nearest three output vectors that the nodes of the triangle containing the reference vector changes from one region to another, it may induce an output vector abrupt change. In addition we need to calculate the switching sequences and switching time of the states at every change of the reference voltage location. In this paper, a new method is proposed in which the three level inverter is decomposed into six space vector diagrams of two level inverters. This modification can reduce considerably the computational time and reduce the algorithm complexity.

3.1) correction of reference voltage vector

Having the location of a given reference voltage vector, one hexagon is selected among the six small hexagons that contain the three level space vector diagram. Each hexagon is identified by a number s defined as given by:

$$s = \begin{cases} 1 \text{ si } \frac{-\pi}{3} \le \theta \le \frac{\pi}{3} \\ 2 \text{ si } \frac{\pi}{3} \le \theta \le \frac{\pi}{2} \\ 3 \text{ si } \frac{\pi}{2} \le \theta \le \frac{5.\pi}{6} \\ 4 \text{ si } \frac{5.\pi}{6} \le \theta \le \frac{7.\pi}{6} \\ 5 \text{ si } \frac{7.\pi}{6} \le \theta \le \frac{3.\pi}{2} \\ 6 \text{ si } \frac{3.\pi}{2} \le \theta \le \frac{11.\pi}{6} \end{cases} \quad (7)$$

After selection of one hexagon, we make a translation of the reference vector V_s^* towards the center of this hexagon.

TABLE III
CORRECTION OF REFERENCE VOLTAGE VECTOR

Hexagon	$V_d^{*\prime}$	$V_q^{*\prime}$
1	$V_d^* - 1/2$	V_q^*
2	$V_d^* - 1/4$	$V_q^* - \sqrt{3}/4$
3	$V_d^* + 1/4$	$V_q^* - \sqrt{3}/4$
4	$V_d^* + 1/2$	V_q^*
5	$V_d^* + 1/4$	$V_q^* + \sqrt{3}/4$
6	$V_d^* - 1/4$	$V_q^* + \sqrt{3}/4$

3.2) Determination of dwelling times

Ones the corrected reference voltage$\hat{V}_s^{*\prime}$ and the corresponding hexagon are determined, we can apply the conventional two level space vector PWM method to calculate the dwelling times, the only difference between the two level SVPWM and the three level SVPWM is the factor 2 appearing at the first two equations as shown in this equation:

$$\begin{cases} T_1 = 2 * \left[\dfrac{\left|\overrightarrow{V_s^{*\prime}}\right|.T_s.\sin\left(\frac{\pi}{3}-\alpha\right)}{\sin\left(\frac{\pi}{3}\right)}\right] \\ T_2 = 2 * \left[\dfrac{\left|\overrightarrow{V_s^{*\prime}}\right|.T_s.\sin(\alpha)}{\sin\left(\frac{\pi}{3}\right)}\right] \\ T_3 = T_s - T_1 - T_2 \end{cases} \quad (8)$$

3.3) Conversion and sequence of the switching states

The reference voltage vector $\hat{V}_s^{*\prime}$ is approximated using the nearest three states which are nodes of the triangle containing the vector identified as X, Y and Z. the optimum sequence of these states is selected so as to minimize the total number of switching transitions. It's well known that these sequences should be reversed in the next switching interval for minimum harmonic impact as given in [3].

D. Modeling and command of the induction motor

The mathematical model of the induction motor can be described by the following equations in a synchronously rotation d-q reference frame [4]:

$$\dot{X} = AX + BU \quad (9)$$

Where:

$$X = \begin{bmatrix} I_{ds} \\ I_{qs} \\ \varphi_{dr} \\ \varphi_{qr} \end{bmatrix}, \dot{X} = \begin{bmatrix} \dot{I_{ds}} \\ \dot{I_{qs}} \\ \dot{\varphi_{dr}} \\ \dot{\varphi_{qr}} \end{bmatrix}, U = \begin{bmatrix} V_{ds} \\ V_{qs} \\ 0 \\ 0 \end{bmatrix} \quad (10)$$

Using Laplace transformation, we obtained:

$$\begin{cases} I_{ds} = \dfrac{1}{(R_s + \sigma L_s S)}\left[V_{ds} + \sigma L_s \omega_s I_{qs} - \dfrac{M}{L_r}\varphi_{dr}S + \omega_s \dfrac{M}{L_r}\varphi_{qr}\right] \\ I_{qs} = \dfrac{1}{(R_s + \sigma L_s S)}\left[V_{qs} - \sigma L_s \omega_s I_{ds} - \omega_s \dfrac{M}{L_r}\varphi_{dr} - \dfrac{M}{L_r}\varphi_{qr}S\right] \\ \varphi_{dr} = \dfrac{1}{S}\left[M\dfrac{R_r}{L_r}I_{ds} - \dfrac{R_r}{L_r}\varphi_{dr} - (\omega_s - \omega_r)\varphi_{qr}\right] \\ \varphi_{qr} = \dfrac{1}{S}\left[M\dfrac{R_r}{L_r}I_{qs} - \dfrac{R_r}{L_r}\varphi_{qr} - (\omega_s - \omega_r)\varphi_{dr}\right] \\ \Omega = \dfrac{1}{JS + K_f}(C_{em} - C_r) \\ C_{em} = P\dfrac{M}{L_r}(\varphi_{dr}I_{qs} - \varphi_{qr}I_{ds}) \end{cases} \quad (11)$$

Flux oriented control ensures a decoupling between rotor flux and the torque developed by the induction motor. This is ensured via the control of the two components i_{sd} and i_{sq} of stator vector current. Thus, the model intended for the vectorial control of the induction motor by considering the conditions of orientation of rotor flux ($\varphi_{rq} = 0, \varphi_{rd} = \varphi_r$) is:

$$\begin{cases} \dfrac{dI_{ds}}{dt} = \dfrac{1}{\sigma L_s}\left(-R_s I_{ds} + \omega_s \sigma L_s I_{qs} + \dfrac{M}{L_r}\varphi_r + V_{ds}\right) \\ \dfrac{dI_{qs}}{dt} = \dfrac{1}{\sigma L_s}\left(-R_s I_{qs} - \omega_s \sigma L_s I_{ds} - \dfrac{M}{L_r}\omega_s\varphi_r + V_{qs}\right) \\ \omega_s = \omega_r + \dfrac{M.i_{qs}}{T_r\varphi_r} \\ i_{qs} = \dfrac{L_r C_{em}}{pM\varphi_r} \\ \dfrac{d\Omega_r}{dt} + K_f\Omega_r = C_{em} - C_r \end{cases} \quad (12)$$

Where:

(Ids, Iqs): Stator current components,
(Vds, Vqs): Stator voltage components,
(Rs, Ls): Stator resistance and inductance,
(Rr, Lr): Rotor resistance and inductance rotor,
M: Mutual inductance,
J: Total inertia,
Cem : Electromgnetic torque,
Cr : Resistive torque,
K_f: Viscousfriction coefficient,
σ : Blondel coefficient,
Ωr: Rotor speed,
$\boldsymbol{\omega_s}$: Stator pulsation,
$\boldsymbol{\omega_r}$: Rotor pulsation.

In this work, we use the indirect method and we go carried out the replacement of the traditional regulator speed by a fuzzy logic regulator as shown on Fig 27. The internal structure of fuzzy logic regulator is given in Fig 7.

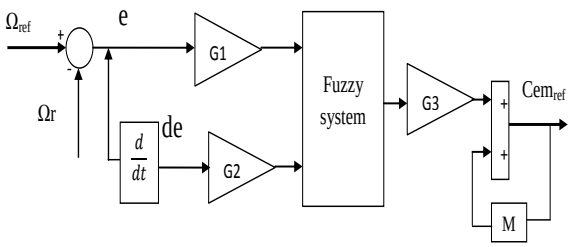

Fig.7 Internal structure of fuzzy regulator for motor speed.

The inputs of the regulator are:

$$E(k) = G_1\left(\Omega_{ref}(k) - \Omega_r(k)\right) \quad (13)$$

$$dE(k) = G_2\frac{E(k+1) - E(k)}{te} \quad (14)$$

The output is the increment of the reference torque:

$$C_{em}{}^*(k) = C_{em}{}^*(k-1) + G_3\Delta C_{em}(k) \quad (15)$$

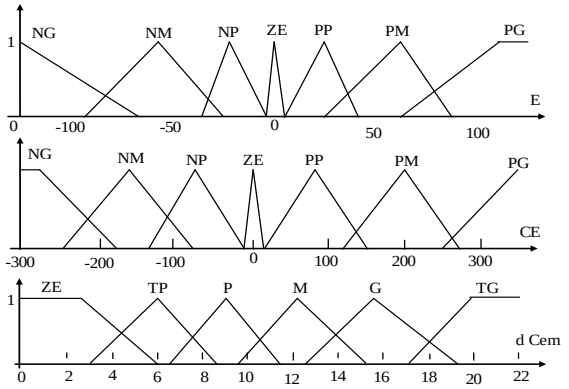

Fig.8 Membership function of each variable.

The fuzzy rules which make it possible to determine the output signal of the regulator according to the input signals are given in table IV:

TABLE IV
FUZZY RULE OF CONTROLLER

E(k) / dE(k)	NG	NM	NP	ZE	PP	PM	PG
NG	TG	TG	G	M	P	TP	ZE
NM	TG	G	M	P	TP	ZE	TP
NP	G	M	P	TP	ZE	TP	P
ZE	M	P	TP	ZE	TP	P	M
PP	P	TP	ZE	TP	P	M	G
PM	P	ZE	TP	P	M	G	TG
PG	ZE	TP	P	M	G	TG	TG

E. Model of the centrifugal pump

The head-flow rate Q-H characteristic of a monocellular centrifugal pump is obtained using Pleider-Peterman model [5, 6]. The multispeed family head-capacity can be expressed approximately by the following quadratic form:

$$HMT = a_0.\Omega_r{}^2 - a_1.\Omega_r.Q - a_2.Q^2 \quad (16)$$

Where:
a_0, a_1, a_2 are constants data by the manufacturer.

The pump torque is given by:

$$C_r = k_r.\Omega_r{}^2 \quad (17)$$

III. RESULTS SIMULATION

In this section, the proposed PV water pumping system is simulated in Simulink-MATLAB. For the sizing of system, we use the analytical model base essentially on the water need evaluation, calculation of the necessary hydraulic energy, determination of the available solar energy as done in [6,7]. Our system in intended to to meet the requirements out of water for a village that's its daily consumption is estimated by 70 m^3 consequently.

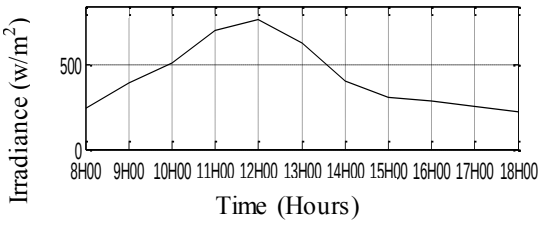

Fig.9 Irradiance profile.

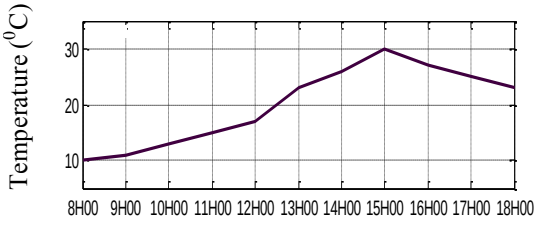

Fig.10 Temperature profile.

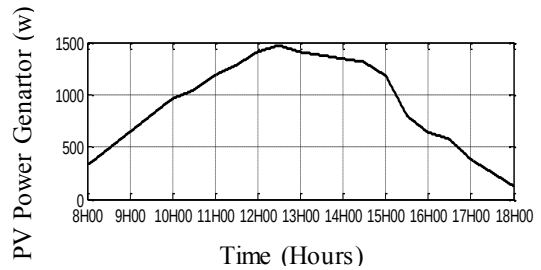

Fig.11 PV power generator (W).

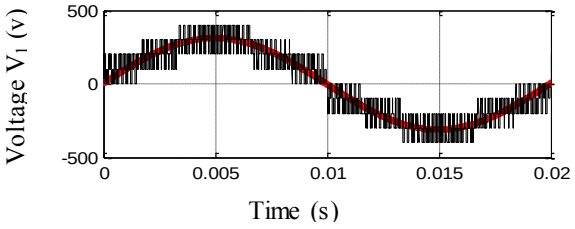

Fig.12 Output voltage of the 3 level DCI (V1).

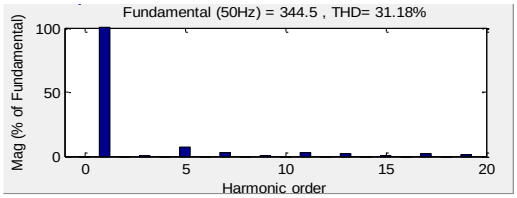

Fig.13 Total harmonic distortion of output voltage.

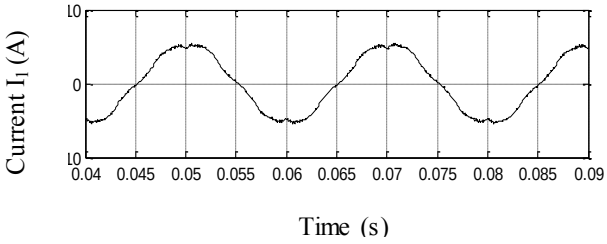

Fig.14 Stator current (A).

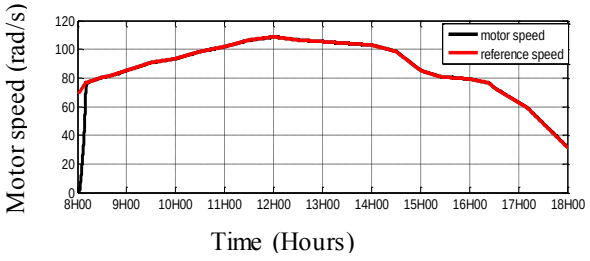

Fig.15 Motor speed.

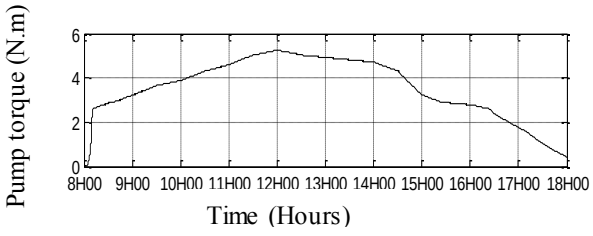

Fig.16 Torque of the pump.

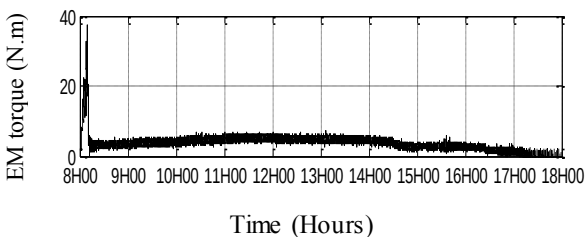

Fig.17 Electromagnetic Torque.

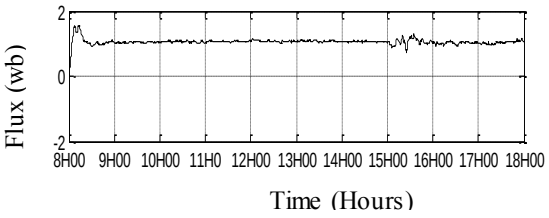

Fig.18 d-axis rotor flux.

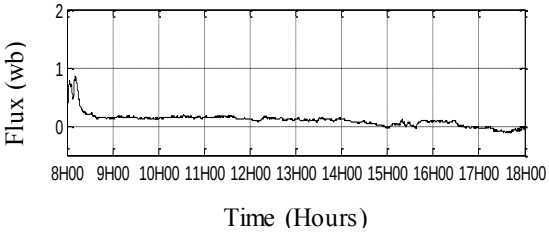

Fig.19 q-axis rotor flux.

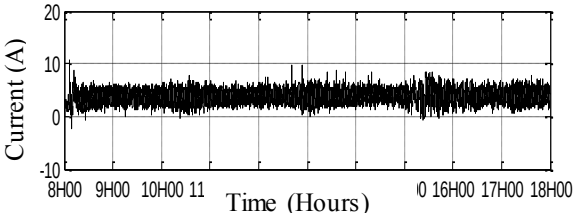

Fig.20 d-axis stator current.

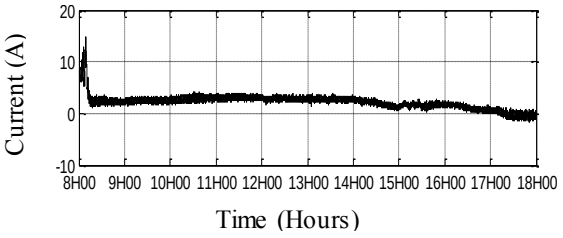

Fig.21 q-axis stator current.

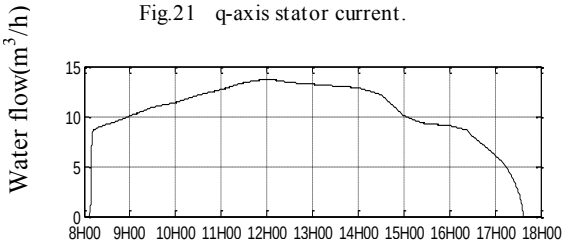

Fig.22 Water flow.

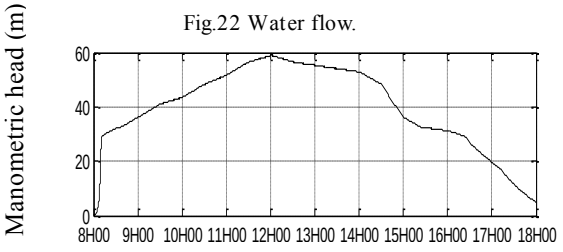

Fig.23 Manometric head of the well (m).

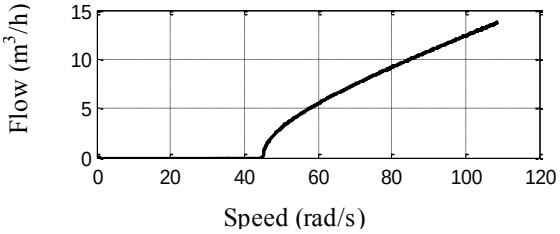

Fig.24 Characteristic Flow-Speed of pump.

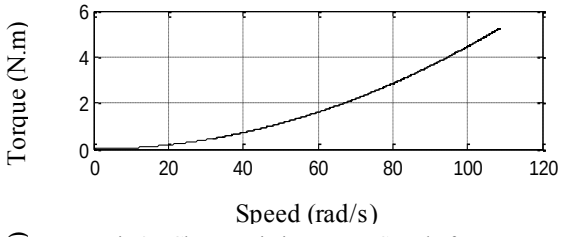

Fig.25 Characteristic Torque-Speed of pump.

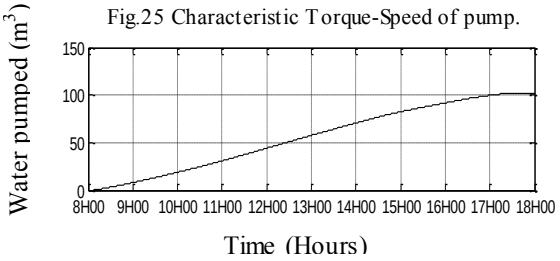

Fig.26 Volume of pumped water.

Characteristics data of PV module	
Maximum point power	60 W
Maximum point voltage	17.1 V
Maximum point current	3.5 A
Temperature coefficients of short circuit current	(0.0065±0.015)A/°C
Temperature coefficients of open circuit voltage	-(80±10) mV/°C
characteristics data of the induction motor	
Stator résistor	0.03552 Ω
Rotor résistor	0.020092Ω
Cyclic inductance of stator	0.0154H
Cyclic inductance of rotor	0.0154H
Mutual inductance	0.0151H
Total inertia	1.25 Kg.m^2
Paire pols number	2
Viscous friction coefficient	0.003915 SI

Regulator	
Current Regulator	
Kp= 0.1066	Ki= 6.3728
Fuzzy Regulator of motor speed	
G_1=0.82	G_2=90 G_3=0.95
Parameters of the centrifugal pump	
Nominal speed	157.85 rad/sec
Pump inertia	0,02 kg.m^2
Nominal flow	21 m^3/h
Nominal heigh	12m
Constant a_0	4,9234.10-3 m/ (rad/sec)^2
Constant a_1	1,58.10^{-5} m(rad/sec(m^2/sec)
Constant a_2	-18144 m/ (m^3/sec)^2

IV. CONCLUSION

This paper proposed the study and the optimization of a water pumping system. On one hand, the PV generator is forced to a maximal power operating by using a fuzzy logic Controller. The results of simulation showed thus the effectiveness of fuzzy logic controller in order to exploit optimal speed to obtain the maximum follow available. On the other hand, for achieving better motor torque generating characteristics, flux oriented control has been introduced in this paper to command the induction motor. A current control scheme combining a decoupling control to achieve a fast dynamic response in a field orientation-controlled induction motor drive was presented in this paper. The induction motor drive with rotor flux, stator current and speed controller has exhibited good transient and steady-state performance. The results show the flux magnitude has been maintained as constant and a torque exhibits a fast response. The motor speed follow it's referential without going beyond showing the effectiveness of the fuzzy controller of the speed what makes it possible to reach the follow and the total head desired.

Also, the three-level diode clamped inverter with its simplified SVPWM improved the quality of the supply voltage of the machine. The simulation results showed that the three-level inverter is the series connection of two two-level inverters and gives low distortion of the output voltage.

V. REFERENCES

[1] H ohm DP, Ropp ME."Comparative study of maximum power point tracking algorithm using anexperimental, programmable, maximum power point tracking test bed". Proc 28th IEEE photovoltaic Specialist Conf 2000; 28:1699–702.

[2] S. M. Ait-Cheikh, « Etude, Investigation et conception d'algorithmes de commande appliqués aux systèmes photovoltaïques». Thèse Doctorat de l'école Polytechnique, 2007.

[3] Lalili D., "Simplified space vector PWM algorithm for three-level inverter with neutral point potential control", The Medeteranean Journal of Measurement and Control", vol 3, No 1, January 2007.

[4] M.F. Mimouni, M.N. Mansouri, B. Benghanem and M. Annabi, 'Vectorial Command of an Asynchronous Motor Fed by a Photovoltaic Generator', Renewable Energy, 29, pp. 433 – 442, 2004.

[5] A. Hamidat, A. Hadj Arab, F. Chenlo and M.A. Abella, 'Performances Costs of the Centrifugal and Displacement Pumps', WREC, pp. 1951 – 1954, 1998.

[6] A. Moussi, A. Betka and B. Azoui, 'Optimum Design of Photovoltaic Pumping System', UPEC99, Leicester, UK, 1999.

[7] I. Narvarte, E. Lorenzo and E. Caamaño, ''PV Pumping Analytical Design and Characteristics of Boreholes'', Solar Energy, Vol. 68, N°1, pp. 49-56, 2000.

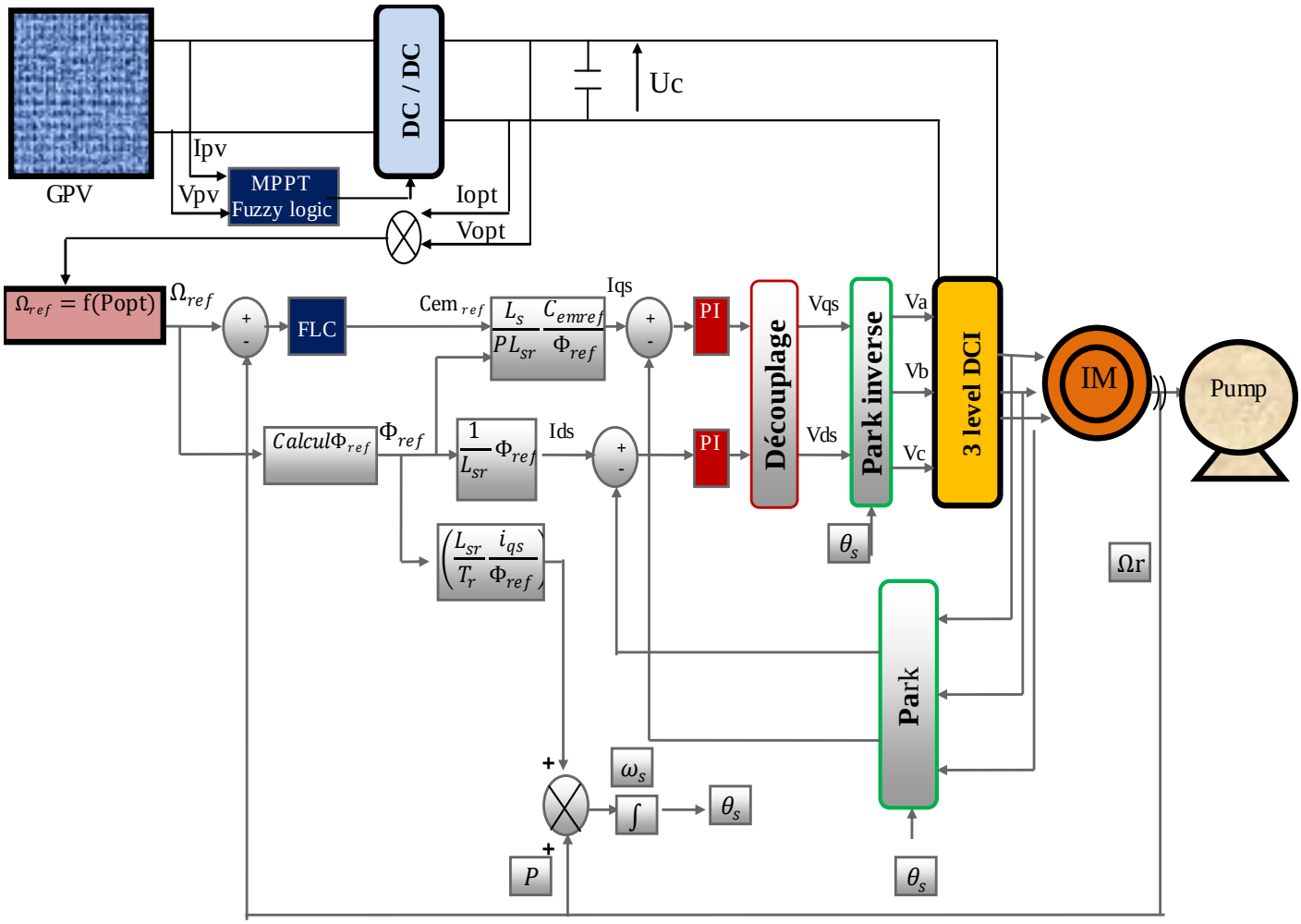

Fig.27 Flux oriented control with regulation of motor speed by a fuzzy logic controller.